

65. S. H. Cadle and S. Bruckenstein, *Anal. Chem.*, **44**, 1993 (1974).
66. T. Takamura and K. Takamura, in "Surface Electrochemistry, Advanced Methods and Concepts," T. Takamura and A. Kozawa, Editors, pp. 222-234, Japan Scientific Societies Press, Tokyo, Japan (1978).
67. T. Takamura, F. Watanabe, and K. Takamura, *Electrochim. Acta.*, **19**, 933 (1974).
68. T. H. V. Setty and H. Wilman, *Trans. Faraday Soc.*, **51**, 984 (1955).
69. J.O'M. Bockris and A. Damjanovic, in "Modern Aspects of Electrochemistry," Vol. 3, J. O'M. Bockris and B. E. Conway, Editors, p. 329, Butterworth London (1964).
70. K. H. Z. Brainina, D. P. Synkova, and I. G. Yudelevich, *J. Electroanal. Chem.*, **35**, 165 (1972).
71. K. H. Z. Brainina, N. K. Kiva, and V. B. Beliavskaia, *Elektrokhimiya*, **1**, 311 (1965).

## Electrolytic Recovery of Gallium from Dilute Solutions Employing Microelectrodes

R. C. Paciej\*

*Naval Air Development Center, Warminster, Pennsylvania 18974*

G. L. Cahen, Jr.,\* and G. E. Stoner\*

*Department of Materials Science, University of Virginia, Charlottesville, Virginia 22901*

E. Gileadi\*

*Department of Chemistry, Tel Aviv University, Ramat Aviv 69978, Israel*

### ABSTRACT

The recovery of gallium from dilute solutions is known to be slow and inefficient due to competing hydrogen evolution and the limitations of mass transport. Methods used to improve the process include pulse plating, inhibition of hydrogen evolution by suitable additives, increasing the pH, and conducting the process at temperatures above the melting point of gallium. In the present work, an alternative approach was taken employing microelectrodes to enhance the rate of mass transport and thus to increase the rate of gallium recovery. Potentiostatic plating and stripping experiments were performed using electrodes ranging in diameter from 1 cm down to 45  $\mu\text{m}$ . The effect of electrode diameter on the rate and efficiency of the plating of gallium was studied at different potentials and under different conditions of mass transport. The effect of plating time was also determined, and the conditions for the optimum recovery of gallium in terms of the overall rate as well as the current efficiency were evaluated. Carbon fiber epoxy composites can serve as ensembles of microelectrodes. It was shown that, with a typical radius of 3-5  $\mu\text{m}$  for the individual fibers, considerable enhancement of the rate of recovery of metals from dilute solutions can be expected.

Novel electrode designs have been suggested in recent years for the recovery of metals from dilute solutions, either as a means for purifying industrial waste, or as a method of primary recovery of the metal from low grade ore. Some well-known designs include the "Swiss roll" (1), the fluidized bed (2), the so-called "Eco cell" (3), as well as various types of porous electrode flow-through cells (4). Most of the above designs cannot be used efficiently for the recovery of gallium due to the low current efficiency caused by hydrogen evolution and because gallium tends to be soluble in the electrolyte used after it has been detached from the electrode surface and is no longer cathodically protected. An alternative electrode design, which has so far not been studied for this purpose, is a microelectrode or an ensemble of microelectrodes on a planar surface.

Recent interest in the electrochemical properties of microelectrodes is due to several possible applications of such systems. They can be considered for implantation in living organisms to follow the changes in concentration of biologically active molecules. The various future applications of microelectrodes were discussed in a recent symposium devoted to this subject (5). A number of theoretical papers have dealt with the calculation of the rate of mass transport to a microelectrode (6-11). In two recent studies (12, 13), the rate of mass transport to ensembles of microelectrodes was calculated, taking into account the interaction of the diffusion layers of adjacent electrodes. It was shown (13, 14) that an added advantage of ensembles of microelectrodes, as compared to large continuous electrodes, is the reduced ohmic potential drop. A number of experimental studies employing microelectrodes of

\*Electrochemical Society Active Member.

various types have been reported in recent years (15-23). Further possibilities for such experimental studies are enhanced by the advent of modern techniques of microelectronics and by the introduction of carbon fiber epoxy matrix composite materials as electrodes in certain applications (19, 24-26).

The inherent advantage of ensembles of microelectrodes for the recovery of metals from dilute solutions is the enhancement of mass transport, as compared to planar electrodes of equal total area. Since the partial current for metal recovery from dilute solutions will usually be limited by mass transport, enhancing the rate of mass transport should increase both the rate of metal recovery and the current efficiency for recovery (assuming that the competing reaction, which is typically hydrogen evolution, is not limited by mass transport). A possible drawback of microelectrodes is their tendency to be easily blocked by impurities and specifically by minute gas bubbles formed in the accompanying reaction of hydrogen evolution. This may lead to a significant scatter of experimental results in laboratory experiments, but should be of lesser importance in large-scale industrial operations in which flow rates of the solutions are typically high and large ensembles of microelectrodes will be used in any one reactor.

### Theory

The limiting current density on a planar electrode following a potential step was given (8) for  $(\pi Dt)^{1/2} \leq r$  as

$$I = nFCD \left[ \frac{A}{\sqrt{\pi Dt}} + \frac{P}{2} \right] \quad [1]$$

in which  $C$  is the bulk concentration,  $A$  is the area, and  $P$  is the circumference of the electrode. By setting  $A = \pi r^2$  and  $P = 2\pi r$ , for a disk electrode this equation reduces to the well-known equation of the limiting current to a spherical electrode

$$I = nFCDA \left[ \frac{1}{\sqrt{\pi Dt}} + \frac{1}{r} \right] \quad [2]$$

The first term in the brackets represents the classical Cottrell equation and is valid at short times when the diffusion layer thickness  $\delta = (\pi Dt)^{1/2}$  is small with respect to the radius  $r$  of the microelectrode. If diffusion is the only mode of mass transport, the time-dependent term in Eq. [1] and [2] will approach zero at long times and the current will be governed by the radius of the microelectrode. This, however, is not a case of practical interest, since in any electrochemical reactor the diffusion layer thickness at steady state is governed by the conditions of flow near the electrode surface. Such steady state is reached when the naturally growing diffusion layer reaches the thickness enforced by electrolyte flow. If the latter is known, the time to reach steady state can readily be estimated from the relationship  $t = \delta^2/\pi D$ .

In the present work, the case studied was that in which the diffusion layer was determined by the method of stirring of the solution. In this case, one can define a capture area, shown in Fig. 1, as the envelope within which the concentration of the reactants and products significantly deviate from their respective bulk values. From simple geometrical considerations, it can be seen that the "capture area"  $A_c$  defined above is related to the diffusion layer thickness and the radius of the microelectrode. The ratio between the capture area and the area of the microelectrode is given by

$$A_c/A_e = 1 + \pi\delta/r + 2\delta^2/r^2 \quad [3]$$

This ratio may serve as a qualitative measure of the enhancement of mass transport to a microelectrode or to an ensemble of microelectrodes. For an infinitely large planar electrode, the above ratio is, by definition, equal to unity. As the ratio between the diffusion layer thickness and the radius of the microelectrode increases, the second and the third terms in the above equation become predominant. When the ratio is very large, the term involving the square of this ratio is most important. With this concept, the enhancement of the rate of diffusion is to an extent proportional to the ratio of areas of a circle having a radius equal to the diffusion layer thickness to the area of the microelectrode. A similar result was reached for an ensemble of microelectrodes assuming that the rate of mass transport was controlled only by diffusion, with no convective flow (13, 14).

### Experimental

**The cell and electrodes.**—A rectangular cell constructed of polymethylmethacrylate was employed. The distance between the working and counterelectrodes was 8.5 cm, and a saturated calomel reference electrode (SCE) was situated in the compartment with and at a distance of 3.5 cm from the working electrode. All potentials shown in this

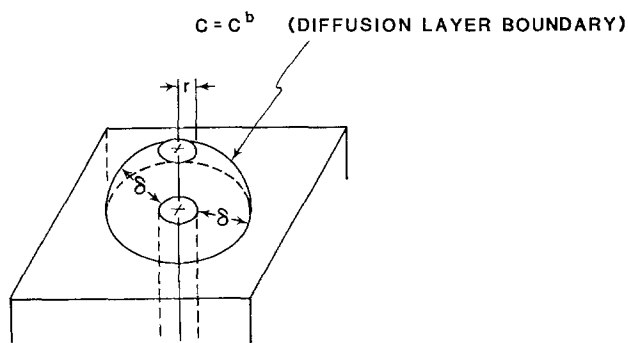


Fig. 1. The capture envelope

paper are with respect to the saturated calomel electrode. The counterelectrode and working electrode compartments were separated by a 125  $\mu\text{m}$  Tyvek separator in order to prevent oxygen from getting to the working electrode when it was polarized cathodically. A 1  $\text{cm}^2$  copper plate was used as the continuous or plate electrode. Copper wires embedded in an epoxy matrix were used as the microelectrodes. The diameters of these electrodes were 1000, 510, 250, 100, 67, and 45  $\mu\text{m}$ . For the three larger sizes, single electrodes were used. For the three smaller sizes, ensembles of electrodes having 6, 13, and 15 electrodes, respectively, were employed. The electrodes were situated at a relatively large distance from each other to ensure that their diffusion layers would not overlap during the experiment. Bonding of the microelectrodes to the embedding polymer initially posed some problems. These were overcome by the use of a silane coupling agent prepared by mixing 5 ml of organosilane ester (Union Carbide, A 176) with 5 ml acetic acid and diluting with 5 ml of distilled water.

After imbedding the copper wires into the polymer, the electrodes were polished to be flush with the surface. Polishing was performed with successively finer polishing materials, starting with 180, 320, 400, and 600 grit papers (3M Company), followed by 10 and 5  $\mu\text{m}$  SiC papers (Mager Scientific Company). In the final polishing stage, 6 and 1  $\mu\text{m}$  diamond pastes were used, followed by 0.05  $\mu\text{m}$  alumina powder (Buehler).

**Electrolyte and methods of stirring.**—The electrolyte was prepared from reagent grade NaOH (Fisher Scientific, 283 g/liter) and anhydrous  $\text{Ga}_2(\text{SO}_4)_3$  (Alfa Products, 2 g/liter, dissolved in distilled water). The molar concentrations were 7.07M hydroxide and 9.4 mM gallium, in the form of the gallate ion  $\text{GaO}_3^{-3}$ . The pH of the solution was 15.1 (27).

Two methods were used to agitate the solution. In initial measurements, a magnetic stirrer was employed. This was found to be unsatisfactory, since hydrogen bubbles sticking to the electrode surface were not removed. Much more efficient stirring was achieved by the use of an impinging jet of electrolyte, which was positioned 1.5 cm above and 0.5 cm away from the working electrode. The effective value of the diffusion layer thickness, estimated from measurements on the plate electrode (see Results and Discussion) was 68 and 19  $\mu\text{m}$  for the two methods of stirring, respectively. The great advantage of the impinging jet was that it helped remove most of the hydrogen bubbles from the surface of the microelectrodes.

**Procedure and apparatus.**—At the start of each set of experiments, the solution was deaerated with pure nitrogen for 30 min. The working electrode was maintained at a potential of  $-1.4\text{V}$  to protect it cathodically. All experiments were conducted potentiostatically using a PAR Model 173 potentiostat. Plating was conducted for 10, 30, and 50s at potentials ranging from  $-1.70$  to  $-1.90\text{V}$ . Anodic stripping was performed at a potential of  $-0.75\text{V}$ , until the anodic stripping current decayed to zero. The charge during plating and anodic stripping was measured with a bipolar computing coulometer (Electrosynthesis Company, Model 680). The amount of gallium stripped off was also measured in some of the experiments by determining the weight loss which varied from the coulometric determinations by no more than  $\pm 5\%$ .

A peristaltic pump (Cole-Palmer Instruments Company) was used to form the impinging jet. It provided a volume flow rate of 9.6 ml/s and a linear flow velocity of ca. 5m/s.

### Results and Discussion

**The rate of gallium deposition.**—The average rate of gallium deposition is shown in Fig. 2 as a function of potential for microelectrodes of different size. In this figure, the current densities are based on the electrode conductors' apparent area with the data for the 1  $\text{cm}^2$  plate electrode shown for comparison. The results for the two largest microelectrodes studied here are not included in

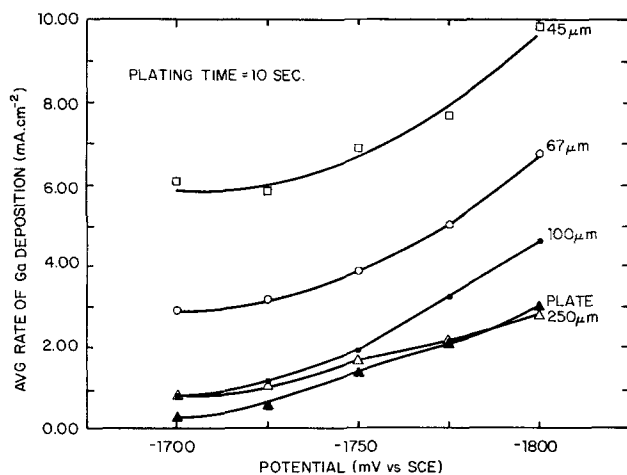


Fig. 2. The effect of the diameter of the electrodes and the potential on the rate of deposition of gallium.

Fig. 2, since they are the same as for the plate electrode. The diffusion-limited current density for gallium deposition was estimated from the current density and the current efficiency measured in the range of potentials of  $-1.8$  to  $-1.9$  V. On the plate electrode, the value obtained in this manner was  $i_L = 4.5$  mA/cm<sup>2</sup>. This value was used to calculate the diffusion layer thickness  $\delta$ , given here. The viscosity of the solution is approximately 6.0 cP, and the diffusion coefficient for the gallate ion is  $D = 3 \times 10^{-6}$  cm<sup>2</sup>/s, significantly lower than in dilute aqueous solutions. Thus, the rate of gallium deposition was under mixed activation/mass-transport control on the plate electrode up to a potential of  $-1.80$  V and switched to fully mass-transport control at more negative potentials. Due to significant enhancement of the rate of mass transport on the microelectrodes, the rate of gallium deposition was probably under mixed control throughout the range of potentials studied.

If we were to assume that the reaction is under mass-transport control for all electrodes at all potentials measured, it would be easy to calculate the difference between the current densities on the plate and on the microelectrodes, since

$$i_L(\text{micro}) - i_L(\text{plate}) = nFDC \left[ \left( \frac{1}{\delta} + \frac{1}{r} \right) - \frac{1}{\delta} \right] = nFDC \left( \frac{1}{r} \right) \quad [4]$$

The differences calculated in this way amount to 3.8, 2.5, 1.7, and 0.7 mA/cm<sup>2</sup> for the 45, 67, 100, and 250  $\mu\text{m}$  diam electrodes, respectively. The average values observed at the less negative potentials are 3.7, 2.5, and 1.7 mA/cm<sup>2</sup>, respectively, the values for the 250  $\mu\text{m}$  electrode being within experimental error of the value for the plate electrode. It is noteworthy, however, that this difference increases at more negative potentials. It is reasonable to assume that in this region the plate electrode is already completely under mass-transport control, while the rate of gallium deposition still increases slightly with increasing negative potential on the microelectrodes.

The solution resistance may play an important role in determining the rate of gallium deposition at the less negative potentials. Since the reversible potential for the deposition of gallium in the solvent is close to  $-1.70$  V, a small difference in the potential across the interface, caused by an IR drop, may effect the rate of deposition of gallium in a major way. As pointed out above (13, 24), the solution resistance (for a fixed value of the current density) decreases with decreasing radius of the microelectrode. This may explain the relatively large difference in current density between the plate electrode and the smallest microelectrode observed in Fig. 2.

It should be noted that the condition  $r \ll \delta$  did not exist even for the smallest microelectrodes employed in this

study. It was shown (12, 13) that for electroanalytical applications the radius of the microelectrodes in the ensemble should be 3  $\mu\text{m}$  or less to have a significant advantage over large electrodes. However, the comparison in that case was done with pulse polarography, which is in itself one of the most sensitive electroanalytical techniques. The present results clearly show that when the radius is decreased below 50  $\mu\text{m}$ , a definite advantage over large electrodes is observed and this advantage increases sharply with decreasing radius. Extrapolating the data in Fig. 2 to a radius of 3–5  $\mu\text{m}$  would indicate a possible increase in the rate of recovery of gallium by one to two orders of magnitude compared to large continuous electrodes. This may be very significant technologically, since the radii of the fibers in graphite fiber epoxy composites are in that range. Thus, graphite fiber composites with relatively low graphite fiber loading may turn out to be very useful as ensembles of microelectrodes for the recovery of metals from dilute solutions.

*Anodic stripping and alloy formation.*—Anodic stripping was conducted following each plating experiment. The potential was held at  $-0.750$  V until the anodic current decayed to zero, and the charge passed in this period was determined with the aid of a coulometer. Some typical anodic stripping curves are shown in Fig. 3. The longer the plating time, the longer the plateau during stripping. It should be noted that a Cu/Ga alloy was formed during longer periods of plating, leading to a somewhat complex form of the anodic stripping transient.

The formation of an alloy is indicated in Fig. 4. The lines shown represent consecutive cathodic plating transients, each followed by anodic stripping, as outlined above. The current density increases after each plating cycle and the current efficiency decreases, showing that the increase in current density is due to an enhancement of the rate of hydrogen evolution. The surface could be restored to its original form (i.e., all the alloy could be removed) by setting the potential at a much more positive value of 0.00 V for a short time following anodic stripping at  $-0.75$  V. It was not maintained at this potential for any length of time, since some anodic dissolution of copper could occur.

*Current efficiency.*—Plots of the average current efficiency for gallium deposition as a function of potential are shown in Fig. 5 for different sized microelectrodes. For the plate and the two largest microelectrodes, the efficiency is low at  $-1.70$  V, has a broad maximum between  $-1.75$  and  $-1.80$  V, and decreases somewhat at higher negative potentials. This behavior is easy to understand. At the lowest negative potentials, one is close to the reversible potential of gallium deposition, and its rate is low and rising slowly (in a linear rather than exponential form) with potential. As the potential reaches  $-1.75$  V, both the gallium deposition and the hydrogen evolution are in the Tafel region and the two partial currents increase to the same extent with potential, leaving their ratio, which is proportional to the current efficiency, essentially constant. It should be noted that the size of the

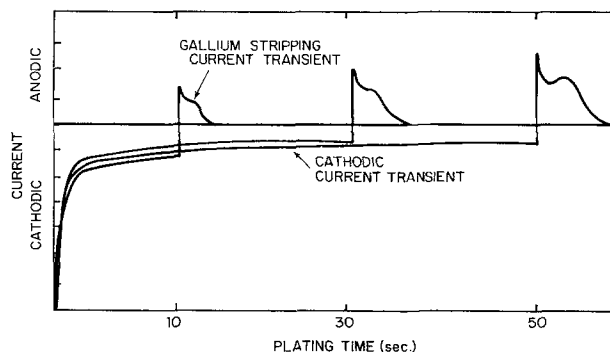


Fig. 3. Three cathodic deposition and following anodic dissolution transients.

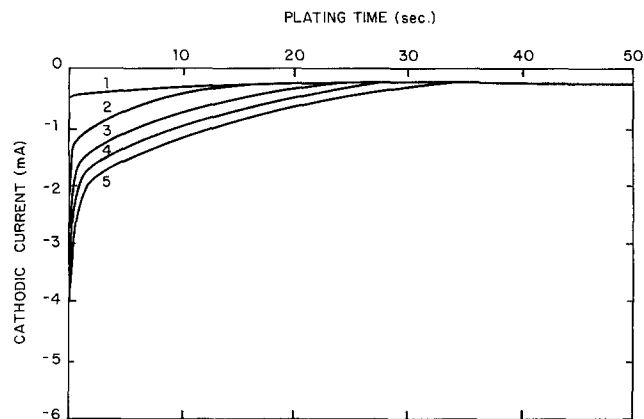


Fig. 4. Consecutive cathodic deposition transients, each followed by anodic stripping. The average current efficiencies (%) were 1-27.6, 2-21.4, 3-17.4, 4-14.7, and 5-13.0.

electrodes has no effect in this range since their radii are large compared to the diffusion layer thickness under the present experimental conditions. The results shown for the smaller microelectrodes ( $250 \mu\text{m}$  or less) are more difficult to reconcile with theory. *A priori*, one might have expected the efficiency to increase with decreasing radius of the microelectrode, since gallium deposition is under partial mass-transport control and its rate should increase with decreasing size, while hydrogen evolution is under activation control and hence should not be effected by the size of the electrode. This view, however ignores the effect of IR drop in solution. This can be estimated by considering the partial current densities for hydrogen evolution shown in Fig. 6. The apparent Tafel slopes observed are quite high, in the range of 0.20-0.25V. If one assumes that the correct Tafel slope should be 0.12V, the experimental data can be corrected by making  $R_{\text{soln}} = 4.5 \Omega \text{ cm}^2$  for the plate electrode and  $0.3 \Omega \text{ cm}^2$  for the microelectrode. While these numbers should only be considered as approximate, they show clearly the important effect of decreasing IR at microelectrodes. It should also be noted that a preliminary estimate of  $R_{\text{soln}}$ , based on the known geometry of the cell and the conductivity of the solution ( $0.38 \text{ mho cm}^{-1}$ ), yielded a value of  $9.0 \Omega \text{ cm}^2$  for the plate electrode. For a spherical electrode of the same diameter as the microelectrode used here, a value of  $0.011 \Omega \text{ cm}^2$  is calculated, significantly lower than found for the flat disk microelectrode, as expected.

The rate of gallium deposition is partially diffusion controlled and is hence little effected by the decrease in solution resistance. As the radius of the microelectrode is decreased, both partial current densities increase, although for different reasons. The diffusion-limited cur-

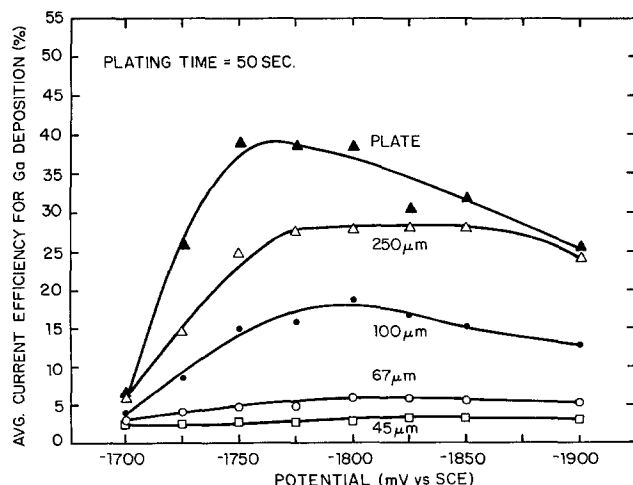


Fig. 5. The effect of the diameter of the electrodes and the potential on the average current efficiency for gallium deposition.

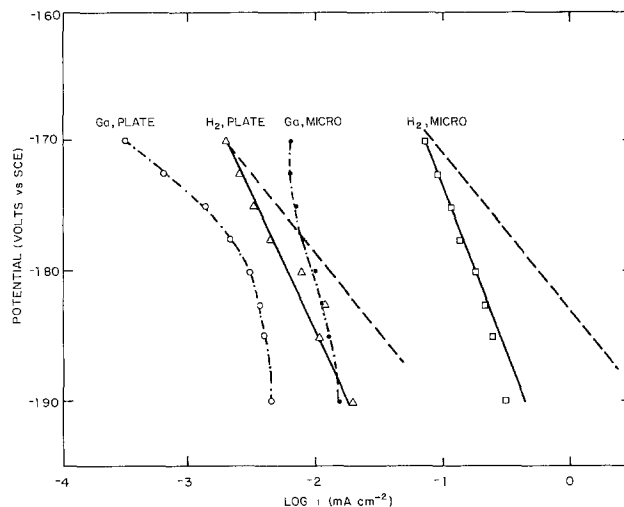


Fig. 6. Partial current densities for hydrogen evolution and for gallium deposition on a plate electrode and on the smallest microelectrodes used in this study ( $r = 22.5 \mu\text{m}$ ). Dotted lines are obtained by assuming  $R = 4.5$  and  $0.30 \Omega \text{ cm}^2$  for the plate and the microelectrode, respectively.

rent density for gallium deposition increases as expected according to Eq. [1] and [2]. At the same time, the IR drop in solution is decreased (13, 14), leading to an increased rate of hydrogen evolution. The latter can depend on a number of factors, including cell geometry and the conductivity of the electrolyte. The results shown in Fig. 5 evidently indicate that in the present experiment the latter effect was predominant.

The large increase of current density for hydrogen evolution for the microelectrodes shown in Fig. 6 cannot be explained on the basis of the change in solution resistance alone. It is probably a catalytic effect occurring at the boundary between the metal and the surrounding epoxy matrix and silane binder. (It could be, for example, that gallium cannot wet this region, leaving a free copper surface on which hydrogen evolution can occur much faster). This effect has not been studied quantitatively.

It is of interest to consider the way in which the two partial current densities would change with a further decrease in the size of the microelectrode. When  $\delta/r$  is very large, the partial current for gallium deposition increases as  $1/r$  without limit, according to Eq. [2]. The solution resistance for unit area tends to zero under these conditions, but this can increase the hydrogen evolution rate only to the value corresponding to the Tafel line in Fig. 6. Thus one would expect that the current efficiency would go through a minimum at a certain value of the diameter of the microelectrode, and then increase with further decreases in diameter. The size of the microelectrode for which this minimum will occur depends on experimental conditions, as pointed out above. It is indeed possible that the smallest microelectrodes used in this study fall in the region of this minimum, since the radius of  $22.5 \mu\text{m}$  was not sufficiently small, compared to the diffusion layer thickness, to cause a very large increase in diffusion-limited current density, as seen from Eq. [2].

### Conclusions

Electrolytic recovery of gallium from dilute solutions in concentrated alkaline has been demonstrated experimentally. The rate of recovery (*i.e.*, the partial current density for gallium deposition) was found to be higher on microelectrodes than on large plate electrodes. This result is particularly significant in view of the fact that the microelectrodes were not really very small, the radius of the smallest being only  $22.5 \mu\text{m}$ , about the size of the diffusion layer thickness. It was shown recently (13, 27) that ensembles of microelectrodes would become very effective, compared to large electrodes, only when the radius of each microelectrode was of the order of  $3 \mu\text{m}$  or even less. This is true when the ensemble is considered for

electroanalytical applications and its performance is compared to pulse polarography, which is itself a powerful tool in electroanalytical chemistry. For metal recovery, it was shown in the present work that the advantage of ensembles of microelectrodes becomes apparent already when the radius of each microelectrode is 50  $\mu\text{m}$  and their relative efficiency increases sharply as the radius decreases further. Carbon fibers used in fiber epoxy composites have radii in the range of 3-5  $\mu\text{m}$ . Thus, a carbon fiber epoxy matrix composite with low fiber loadings (to comply with the requirement that the diffusion layers of adjacent electrodes will not overlap) could serve as a very good and relatively inexpensive ensemble of microelectrodes, which would be highly effective for the recovery of metals from dilute solutions. An effort to fabricate such composite electrodes or other types of ensembles of microelectrodes having even smaller radii of the individual microelectrodes is fully justified in view of their possible application for the recovery of metals and for the purification of industrial effluents containing heavy metal contaminants.

The decrease in current efficiency with decreasing diameter needs further investigation. If this is indeed due to a decrease of the IR drop in solution, as suggested above (12, 13), the current efficiency should reach a minimum, dependent on cell configuration and specific conductivity of the solution, and rise thereafter steadily with decreasing radius, after solution resistance has become insignificant. If the hydrogen evolution reaction is enhanced on the microelectrodes for some other reason (e.g., due to the reduction in the nucleation overpotential associated with hydrogen bubble formation at the edges of the microelectrodes), then an increase of the current efficiency with decreasing radius of the microelectrode may not be observed. In such event, one may still take advantage of the enhanced rate of gallium deposition on ensembles of microelectrodes, combined with suitable highly effective hydrogen inhibitors, to further identify conditions for high rate, high efficiency recovery of the metal from dilute solutions.

#### Acknowledgment

This work was supported in part by the National Science Foundation under NSF Grant CPE-8119765.

Manuscript submitted Dec. 10, 1984; revised manuscript received Feb. 11, 1985.

*The University of Virginia assisted in meeting the publication costs of this article.*

#### REFERENCES

1. P. M. Robertson, B. Scholder, G. Theis, and N. Ibl, *Chem. Ind.*, 459 (1978).
2. G. Van Der Heiden, C. M. S. Rauts, and H. F. Boon, *ibid.*, 465 (1978).
3. F. S. Holland, *ibid.*, 458 (1978).
4. D. Matic, *J. Appl. Electrochem.*, **9**, 15 (1979).
5. Symposium on Ultramicroelectrodes, The Electrochemical Society Meeting, Cincinnati, Ohio, May 6-11, 1984; see Abstracts 382-395, pp. 521-537, The Electrochemical Society Extended Abstracts, Vol. 84-1, Cincinnati, OH, May 6-11, 1984.
6. R. M. Wightman, *Anal. Chem.*, **53**, (9) (1981).
7. O. S. Ksenzhek and G. A. Lobach, *Elektrokhimiya*, **17**, 266 (1981).
8. K. B. Oldham, *J. Electroanal. Chem.*, **122**, 1 (1981).
9. J. B. Flanagan and J. Marcous, *J. Phys. Chem.*, **77**, (8) (1973).
10. K. Aiki and J. Osteryoung, *J. Electroanal. Chem.*, **122**, 19 (1981).
11. T. Gueshi, K. Tokuda, and H. Matsuda, *ibid.*, **89**, 247 (1978).
12. H. Reller, E. Kirowa-Eisner, and E. Gileadi, *ibid.*, **138**, 65 (1982).
13. H. Reller, E. Kirowa-Eisner, and E. Gileadi, *ibid.*, **161**, 247 (1984).
14. H. Reller, Ph.D. Dissertation, Tel-Aviv University, Tel Aviv, Israel (1984).
15. H. A. Laitinen and I. M. Kolthoff, *This Journal*, **61**, 3344 (1939).
16. C. R. Iro, S. Asakura, and K. Nobe, *ibid.*, **119**, 698 (1972).
17. J. C. Myland and K. B. Oldham, *J. Electroanal. Chem.*, **147**, 295 (1983).
18. P. Pint and S. N. Flengas, *This Journal*, **123**, 1042 (1976).
19. L. Nacamulli and E. Gileadi, *J. Appl. Electrochem.*, **12**, 73 (1982).
20. B. Scharifker and J. G. Hills, *J. Electroanal. Chem.*, **130**, 81 (1981).
21. A. J. Bard, *Anal. Chem.*, **33** (1961).
22. T. Pavlopoulos and T. D. H. Strickland, *This Journal*, **104**, 116 (1957).
23. M. A. Dayton, J. C. Brown, K. J. Stutts, and R. M. Wightman, *Anal. Chem.*, **52**, 946 (1980).
24. G. Stafford, Ph.D. Dissertation, University of Virginia, Charlottesville, VA (1981).
25. M. Sachyani, M.Sc. Dissertation, Tel-Aviv University, Tel Aviv, Israel (1980).
26. G. E. Stoner, G. L. Cahen, Jr., M. Sachyani, and E. Gileadi, *Bioelectrochem. Bioenergetics*, **9**, 229 (1982).
27. H. S. Harned and B. B. Owen, "Physical Chemistry of Electrolytic Solutions," ACS Monograph, American Chemical Society, Washington, DC (1958).
28. H. Reller, E. Kirowa-Eisner, and E. Gileadi, Abstract 392, p. 532, The Electrochemical Society Extended Abstracts, Vol. 84-1, Cincinnati, Ohio, May 6-11, 1984.
29. J. O. Howell and R. M. Wightman, Abstract 385, p. 525, The Electrochemical Society Extended Abstracts, Vol. 84-1, Cincinnati, Ohio, May 6-11, 1984.